

In Situ Soft X-ray Studies of Ethylene Oxidation Mechanisms and Intermediates on the Pt(111) Surface

Daniel J. Burnett,[†] Aaron M. Gabelnick,[‡] Daniel A. Fischer,[§] Anderson L. Marsh,[‡] and John L. Gland^{*,†,‡}

Department of Chemical Engineering and Department of Chemistry, University of Michigan, Ann Arbor, Michigan 48109, and Materials Science and Engineering Laboratory, National Institute of Standards and Technology, Gaithersburg, Maryland 20899

Received: May 2, 2004

In situ studies of ethylene oxidation on Pt(111) have been performed using a powerful combination of fluorescence yield soft X-ray methods for temperatures up to 600 K and oxygen pressures up to 0.01 Torr. Absolute carbon coverages have been determined both in steady-state and dynamic catalytic conditions on the Pt(111) surface. Fluorescence yield near-edge spectroscopy (FYNES) and temperature-programmed fluorescence yield near-edge spectroscopy (TP-FYNES) experiments above the carbon K edge were used to identify the structure and bonding of the dominant surface species during oxidation. TP-FYNES experiments of preadsorbed ethylene coverages in oxygen pressures up to 0.01 Torr indicate a stable intermediate is formed over the 215–300 K temperature range. By comparing the intensity of the C–H σ^* resonance at the magic angle with the intensity in the carbon continuum, the stoichiometry of this intermediate has been determined explicitly. Based on calibration with known C–H stoichiometries, the intermediate has a C_2H_3 stoichiometry for oxygen pressures up to 0.01 Torr, indicating oxydehydrogenation occurs before skeletal oxidation. FYNES spectra at normal and glancing incidences were performed to characterize the structure and bonding of this intermediate. Using FYNES spectra of ethylene, ethylidyne, and acetylene as reference standard, this procedure indicates the oxidation intermediate is tri- σ vinyl. Thus, oxidation of ethylene proceeds through a vinyl intermediate, with oxydehydrogenation preceding skeletal oxidation.

Introduction

The study of catalytic hydrocarbon oxidation over platinum surfaces is vital in understanding how to reduce the hydrocarbon content in automobile exhaust streams and is important for calorimetric hydrocarbon sensing. Ethylene is an interesting hydrocarbon for oxidation due to its relative simplicity and the limited number of possible oxidation products. The interaction and reaction of ethylene on platinum surfaces remains an active area of research.^{1–26}

On the clean Pt(111) surface below 150 K, ethylene rehybridizes to a sp^3 configuration and forms a di- σ bond to the surface.^{5,7,17} As determined by near-edge X-ray absorption fine structure (NEXAFS) experiments at normal and glancing incidences, this di- σ ethylene species adsorbs with the C–C axis nearly parallel to the Pt(111) surface.^{27–29} Propylene adsorbed on Pt(111) below 150 K also adopts a nearly parallel, di- σ configuration, as determined using NEXAFS.^{30,31}

The saturation concentration of ethylene on Pt(111) below 150 K remains somewhat controversial. Nuclear reaction analysis,¹¹ X-ray photoemission spectroscopy (XPS),⁹ and a combination of high-resolution electron energy loss spectroscopy (HREELS), temperature-programmed desorption (TPD), and ultraviolet photoemission spectroscopy (UPS) experiments¹⁵

indicate a saturation ethylene coverage of 0.25 monolayer. However, other XPS,¹⁰ direct recoil spectroscopy with time-of-flight,³² and elastic recoil detection spectroscopy³³ experiments suggest a 0.50 monolayer saturation coverage. Results presented here indicate a saturation coverage of 0.3 monolayer based on comparison with a saturated coverage of CO.

Heating the adsorbate-covered surface to 300 K causes ethylene (235 K) and hydrogen (250 K) desorption.^{3,16,17} The remaining dehydrogenated species forms a stable intermediate with C_2H_3 stoichiometry.^{1–5,16,17} Using HREELS Ibach and Lehwald first ascribed the ethylidyne ($CH_3-CH\equiv$) structure to this species at 300 K.⁵ Combining HREELS, low-energy electron diffraction (LEED), and thermal desorption spectroscopy experiments, Kesmodel, Dubois, and Somorjai postulated an ethylidyne ($CH_3-C\equiv$) species with the C–C bond nearly perpendicular to the surface.² Recent evidence supports this ethylidyne configuration for adsorbed ethylene on Pt(111) at 300 K.^{4,17,27,28} NEXAFS experiments at normal and glancing angles also indicate ethylidyne is adsorbed with the C–C bond nearly perpendicular to the surface plane.^{27,28}

The reaction of ethylene with oxygen on platinum surfaces has been investigated under ultrahigh-vacuum conditions on low Miller index single crystals^{16–19,26} and at higher pressures on polycrystalline and supported platinum surfaces.^{20–25} On the Pt(111) surface, postexposures of ethylene on an atomic oxygen saturated surface reduce the ethylene coverage to 60% of the saturated ethylene level.¹⁷ There is evidence for two forms of adsorbed ethylene on this atomic oxygen saturated surface.^{17,18,26} Using a combination of EELS and TPD, Steininger et al. were the first to find evidence for a di- σ bonded and weakly adsorbed

* To whom correspondence should be addressed at the Department of Chemistry, University of Michigan. Phone: 734-764-7354. Fax: 734-647-4865. E-mail: gland@umich.edu.

[†] Department of Chemical Engineering, University of Michigan.

[‡] Department of Chemistry, University of Michigan.

[§] National Institute of Standards and Technology.

π bonded ethylene species adsorbed on atomic oxygen layers on Pt(111).¹⁷

The primary reaction products for coadsorbed ethylene and atomic oxygen were H_2O , CO_2 , and CO .¹⁶ Oxidation of ethylene occurs in two steps. The first step involves both oxydehydrogenation and ethylene desorption. Ethylene (235 K) and a small amount of ethane (240 K) desorb. In this same temperature range, C–H reacts with coadsorbed atomic oxygen to form H_2O between 250 and 300 K. Berlowitz et al. suggested the remaining oxidation product has 1:1 C–H stoichiometry.¹⁶ The exact molecular nature of the intermediate was not directly determined, but the authors ruled out any carboxyl or hydroxyl groups and suggested an acetylenic species. Using EELS analysis Steininger, Ibach, and Lehwald identified a stable ethylene oxidation intermediate and ruled out ethynylidyne or any oxygen-containing intermediates.¹⁷ Skeletal oxidation occurs above 330 K, resulting in CO , CO_2 , and further H_2O formation from the remaining hydrogen.¹⁶ Similar sequential oxydehydrogenation followed by skeletal oxidation was recently identified in propylene oxidation on Pt(111). Propylene forms a stable C_3H_5 intermediate with removal of the vinyl hydrogen.³⁴ Studies of propylene and atomic oxygen on a 100 Å Pt/sapphire film also suggest sequential oxydehydrogenation followed by skeletal oxidation.³⁵

This paper is part of a series of in situ studies of simple hydrocarbon, deep oxidation processes on platinum surfaces. Mechanistic studies on propylene and propyne oxidation have recently been concluded on platinum single crystals, foils, and thin films.^{31,35,36} Regarding propyne, a combination of TPRS and fluorescence yield techniques were performed to study propyne oxidation over a wide pressure range.³⁶ Propyne adsorbs nearly parallel to the Pt(111) surface. Regardless of coverage and beginning conditions, TPRS and temperature-programmed fluorescence yield near-edge spectroscopy (TP-FYNES) experiments indicate oxydehydrogenation and skeletal oxidation occur concurrently and the oxidation proceeds with a fixed C_3H_4 stoichiometry in oxygen pressures up to 0.01 Torr.³⁶ Similar results were obtained for acetylene oxidation on Pt(111) in oxygen pressures up to 0.009 Torr, where oxydehydrogenation and skeletal oxidation occur simultaneously over the 330–420 K temperature range.³⁷ TP-FYNES experiments of adsorbed propylene in atmospheres of oxygen indicate a C_3H_5 oxidation intermediate is dominant for oxygen pressures up to 0.02 Torr.³¹ Spectroscopic identification of the C_3H_5 intermediate indicated that the structure of the intermediate is a tri- σ 1-methylvinyl adsorbed with the dehydrogenated C–C bond almost parallel to the Pt(111) surface. Similar sequential oxydehydrogenation was observed during investigations of cyclopropane oxidation on the Pt(111) surface.³⁸ These studies clearly indicate that surface properties and reactant properties both play major roles in controlling oxidation reactions.

Experimental Section

All experiments were conducted on the U7A beam line at the National Synchrotron Light Source (NSLS) at Brookhaven National Laboratory using a fluorescence yield detector optimized for carbon fluorescence.³⁹ The U7A beam line is described in detail elsewhere.³¹

The Pt(111) crystal was oriented within 0.5° of the low-index plane and was mounted on Ta wire supports attached to the end of a 6 ft liquid nitrogen cooled reentrant manipulator. Temperature was measured with a type K (chromel–alumel) thermocouple spot-welded to the back of the crystal. Temperature was controlled using a RHK temperature controller. The Pt(111) crystal was initially cleaned by cycles of Ar^+ sputtering

followed by annealing to 1000 K. Once sulfur was removed via Ar^+ bombardment, the sample was cleaned by heating the crystal to 600 K in 0.002 Torr of O_2 for 60 s. After the oxygen was removed, the crystal was annealed to 1000 K for 20 s. Reactive gases, ethylene (Matheson 99.99%) and acetylene- d_2 (Cambridge Isotopes 99%), were dosed into the background using leak valves. Acetylene- d_2 was used after exchange processes in the gas doser were below 5%. Flow was maintained throughout reactivity experiments using a throttled turbo pump. Oxygen (Matheson, 99.998%) pressures were measured using a capacitance manometer.

Spectra (FYNES experiments) were taken with $150\text{ }\mu\text{m}/150\text{ }\mu\text{m}$ slits, yielding an overall energy resolution of 0.4 eV. The spectra of the adsorbed species were corrected by division with a clean spectrum taken during the same ring fill to remove the detector function from the spectra and minimize the effect of scattered light in the spectra. When analyzing spectra, two normalization techniques, division and subtraction, are used. With low signal-to-noise ratios, division by a clean spectrum is appropriate. With higher signal-to-noise ratios, subtraction of a clean spectrum can be used to normalize the spectra. Comparing the results of these two normalization methods greatly facilitates spectral analysis so that artifacts derived from normalization can be identified. When a peak is manifested using one of the normalization techniques, the peak is investigated further. Close analysis of the 306–310 eV peak (position varies slightly between spectra) in these spectra clearly indicate that this peak is a manifestation of normalization using the division method. No 306–310 eV peak was present when the spectra were normalized by the subtraction method. In analyzing the FYNES data, the carbon edge function was placed at the energy of the XPS maximum of C1s of ethylene on Pt(111) of 285.0 eV plus the work function of Pt(111) with an adsorbed layer of ethylene of 4.2 eV,⁴⁰ yielding a placement of 289.2 eV. FYNES spectra were peak-fitted after subtraction of the carbon step edge using Gaussian functions. Outka and Stöhr comprehensively describe the functional form of the step edge, location of the step edge, determination of the resonance angle, and FYNES peak fitting in general.^{41,42}

All kinetic, or transient, experiments were performed with $450\text{ }\mu\text{m}/450\text{ }\mu\text{m}$ slits yielding a 1.2 eV energy resolution and a fluorescence intensity of 10 000 counts/s for a saturated CO coverage at 330 eV, in the carbon continuum. A 2000 Å, 20% transmittance window inserted immediately upstream of the reaction chamber was used for all in situ reactivity experiments. The window allows reaction chamber pressures up to 10 Torr while maintaining ultrahigh-vacuum conditions upstream of the reaction chamber. All temperature-programmed experiments used a heating rate of 0.5 K/s. Data were averaged over a 4 s interval, yielding a signal-to-noise ratio near 4:1 for a saturated CO coverage. The experimental configuration allows for 2–3 K temperature resolution during the temperature-programmed experiments. Repeated experiments indicate that thermal transitions are reproducible to 2 K. Most transient experiments were done at 330 eV (in the carbon continuum) and at normal incidence. At this energy, the signal is an unambiguous determination of the amount of carbon on the surface. Other energies may be monitored to measure the concentration of specific structural aspects of adsorbed molecules which have well-resolved resonances (i.e. C–H σ^* at 288 eV). Absolute carbon coverages were determined by comparing carbon continuum intensities of the adsorbed hydrocarbons with carbon continuum intensities of a saturated coverage of CO. Because the absolute carbon coverage for a saturated CO coverage is

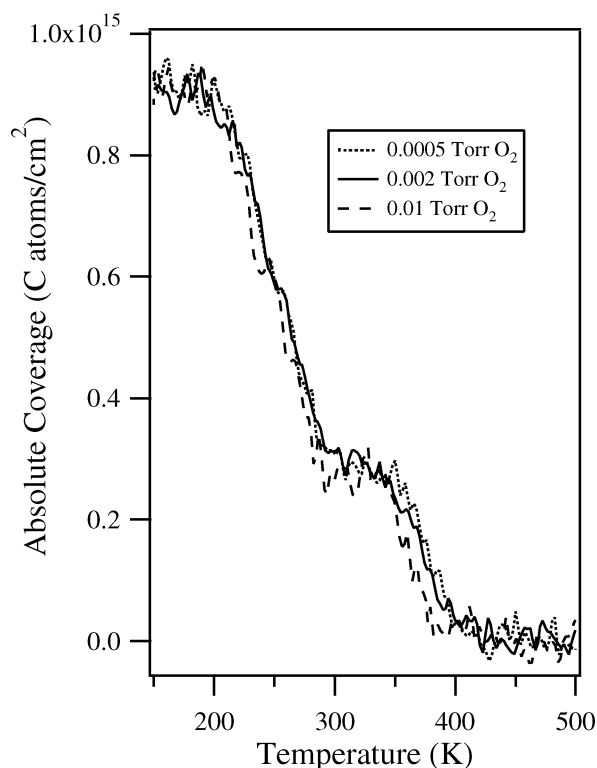


Figure 1. TP-FYNES experiments of a preadsorbed ethylene coverage heated in three pressures of oxygen. A stable oxidation intermediate is formed from 215 to 300 K for all three oxygen pressures. Intensities were measured at 330 eV.

known (0.96×10^{15} CO atoms/cm²),⁴³ absolute surface carbon concentrations are used throughout this paper. Saturated coverage CO fluorescence yields in the carbon continuum (330 eV) were monitored daily to guarantee reproducibility of intensities.

TP-FYNES experiments were conducted in the following manner. First, the crystal was cleaned by heating to 600 K in oxygen and then flashing the temperature to 1000 K to remove atomic oxygen. Once the clean crystal cooled to 150 K, ethylene was dosed via a leak valve while the surface carbon concentration was monitored at 330 eV. When the crystal reached saturation, the leak valve was closed and oxygen was introduced via a leak valve with the ion gauge off. Reaction pressures were achieved using a combination of pump throttling and leak valve control. Once the desired oxygen pressure was reached and stabilized, the crystal was resistively heated from 100 to 600 K at a rate of 0.5 K/s while the fluorescence intensity was monitored.

Results and Discussion

TP-FYNES oxidation experiments of a saturated ethylene coverage heated in oxygen pressures between 0.0005 and 0.01 Torr are displayed in Figure 1. Intensities were measured at 330 eV in the carbon continuum where direct measurements of total carbon concentrations on the surface can be obtained. Calibration of this signal was based on the known coverage of CO on Pt(111), as outlined in the Experimental Section. A saturated ethylene exposure results in a coverage of 0.90×10^{15} carbon atoms/cm² or 0.45×10^{15} ethylene molecules/cm². This corresponds to an ethylene coverage of 0.30 ethylene molecules/platinum atom. This suggests that the absolute coverage of ethylene on Pt(111) is slightly higher than 0.25 platinum monolayer^{9,11,15} as opposed to 0.50 platinum monolayer value proposed by other researchers.^{10,32,33}

When an adsorbed ethylene coverage is heated in oxygen, the carbon concentration remains constant until 215 K, where a precipitous drop in carbon coverage begins and continues until 300 K. This drop in carbon coverage corresponds to ethylene desorption, as indicated by TPRS results of coadsorbed ethylene and atomic oxygen obtained by other researchers.^{16,17} Berlowitz et al. reported ethylene desorption at 235 K on an atomic oxygen covered Pt(111) surface. The difference in temperatures can be attributed to the different heating rates used for the current TP-FYNES experiments (0.5 K/s) and the TPRS work by Berlowitz and co-workers (10.7 K/s). Estimates for the desorption temperature shift between TPRS and TP-FYNES experiments can be obtained using a first-order Redhead method,⁴⁴ yielding a predicted decrease of 18 K with a heating rate of 0.5 K/s. The 217 K desorption temperature predicted using a 0.5 K/s heating rate agrees favorably with the 215 K desorption temperature determined via TP-FYNES experiments. Previous TPRS data indicate water is formed in the temperature range of this first drop in carbon coverage.^{16,17} The onset temperature for ethylene desorption is independent of oxygen pressure. As the temperature increases further, the carbon intensity remains constant at a level of 0.28×10^{15} carbon atoms/cm², indicating that the oxidation intermediate formed by oxydehydrogenation is stable for almost 50 K. Above 345 K the remaining carbon-containing species reacts until the surface is clean by 410 K. The onset temperature for this skeletal oxidation process depends on the ambient oxygen pressure. For 0.01 Torr of oxygen, reaction begins by 345 K, while, in 0.0005 Torr of O₂, reaction does not begin until 360 K. Previous researchers detected carbon dioxide, carbon monoxide, and water formation above 350 K during TPRS experiments of coadsorbed atomic oxygen and ethylene.^{16,17} Thus, the removal of carbon in this temperature range can be associated with skeletal oxidation of the remaining oxidation intermediate.

The comparison of TP-FYNES experiments of saturated ethylene (solid line) with coadsorbed ethylene and atomic oxygen (dotted line) is displayed in Figure 2. The data for both experiments were taken at 330 eV and are in 0.002 Torr of oxygen. For the coadsorbed experiment, oxygen was dosed at 100 K and heated to 250 K, creating a saturated layer of atomic oxygen on the surface.⁴⁵ The crystal was then cooled to 150 K, where ethylene was dosed until the carbon intensity was maximized and stable. The carbon coverage for the coadsorbed atomic oxygen and ethylene corresponds to 0.60×10^{15} carbon atoms/cm² or roughly 66% of a saturated ethylene coverage. This value agrees favorably with the approximate 60% value obtained previously.¹⁷ For the coadsorbed atomic oxygen and ethylene experiment there is an initial drop in carbon coverage around 220 K. This temperature agrees with the ethylene desorption temperature obtained in previous atomic oxygen and ethylene TPRS experiments.^{16,17} As with the saturated ethylene experiment, the carbon intensity drops sharply until 300 K. Above 300 K, the reactions between coadsorbed ethylene and oxygen and ethylene with gas-phase oxygen mirror one another exactly. In both experiments, the carbon intensity remains constant until 350 K, indicating a stable intermediate. Above 350 K the carbon intensity drops until the surface is clean by 410 K. Thus, coadsorbed atomic oxygen appears to only affect the initial amount of ethylene adsorbed on the Pt(111) surface.

TP-FYNES experiments were performed at different well-resolved molecular resonances in order to elucidate the stoichiometry of the stable oxidation intermediate shown in the TP-FYNES experiments (Figures 1 and 2). The magic angle (55°) is used to measure the intensity of molecular resonances

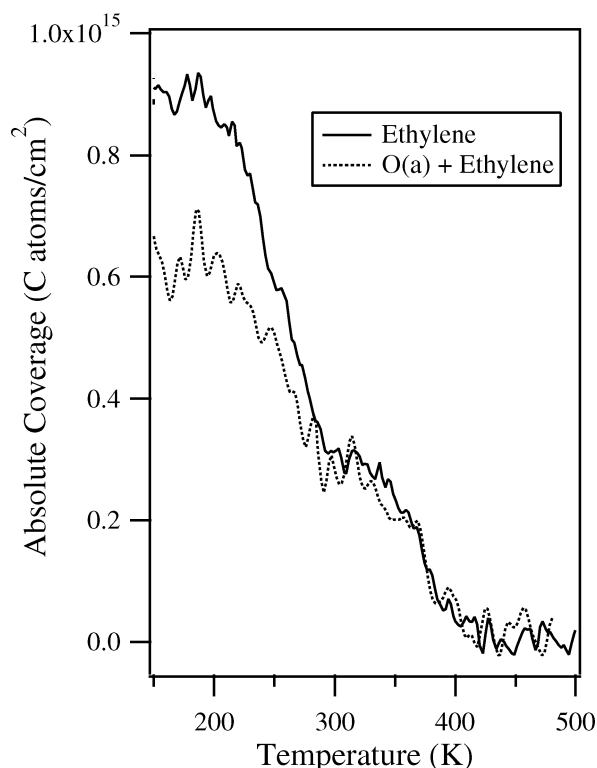


Figure 2. TP-FYNES experiments of ethylene (solid line) and coadsorbed atomic oxygen and ethylene (dotted line) heated in 0.002 Torr of oxygen. Both adsorbed configurations result in formation of a stable intermediate over the same coverage and temperature range. Intensities were measured at 330 eV.

independent of the orientation of the molecule on the surface.⁴¹ A detailed description of this method for determining C–H stoichiometry in situ is available in the literature. This method has been used to determine the intermediate stoichiometry in propylene oxidation on Pt(111).³¹ The intensity of the C–H σ^* resonance, 287.8 eV, at 55° along with the carbon continuum intensity at 330 eV is shown in Figure 3 for a saturated coverage of ethylene heated in 0.002 Torr of oxygen. As shown later in Figures 5–8, the C–H σ^* resonance at 287.8 eV is large and has a consistent position for these hydrogen-rich C_2 species. The C–H σ^* resonance is well-resolved from other molecular resonances and is clearly below the carbon edge (289.2 eV), so the intensity at 287.8 eV is a good measure of the number of C–H bonds. The C–H stoichiometry was calibrated using the stoichiometry of known adsorbates. For both the C–H σ^* resonance and the carbon continuum experiments the intensity remains constant until approximately 215 K, where a sharp drop in intensity begins and continues until 300 K. Both intensities remain constant from 300 to 350 K, where they both begin to decrease again until both resonances reach zero by 410 K. Examination of the initial drop in intensity of the two signals indicates that the C–H σ^* resonance intensity drops more than the 330 eV signal. The C–H stoichiometry is the ratio of these two intensities. With the stoichiometry at 150 K known (C_2H_4), the ratio of the two spectra will indicate any changes in C–H stoichiometry. The inset in Figure 3 displays the C–H σ^* resonance intensity divided by the carbon continuum intensity. This plot clearly indicates that the C–H stoichiometry drops from C_2H_4 at 150 K to C_2H_3 by 300 K. This result is in contrast to TPRS results by Berlowitz et al., where they suggested an acetylenic intermediate with a C–H stoichiometry of 1:1.¹⁶ Exact determination of intermediate stoichiometries can be challenging in TPRS studies, because integration of peak

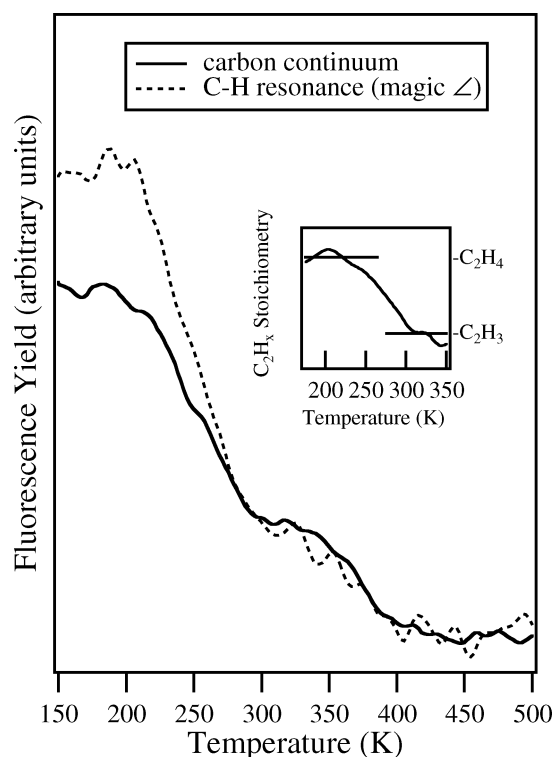


Figure 3. TP-FYNES of ethylene in 0.002 Torr of O_2 taken at the C–H σ^* resonance (dotted line) and carbon continuum (solid line) at the magic angle. The ratio of the two traces (inset) indicates the intermediate at 300 K has C_2H_3 stoichiometry.

intensities is often difficult. Ethylene oxidation is especially challenging because a majority of the adsorbed ethylene desorbs before skeletal oxidation begins.

Similar results were recently obtained for propylene oxidation.³¹ Propylene oxidation also proceeds via an oxydehydrogenated intermediate. The saturated coverage of propylene begins to desorb around 220 K. Compared to ethylene oxidation, a smaller fraction of the propylene desorbs at 220 K. Approximately 40% of the propylene desorbs at 220 K, while almost 70% of the ethylene desorbs at 220 K. Regarding propylene oxidation, a C_3H_5 intermediate is formed over the 250–300 K temperature range, above which skeletal oxidation begins. Spectroscopic studies indicate that the propylene oxidation intermediate is formed by removal of the vinyl hydrogen.³¹ For ethylene oxidation, the C_2H_3 intermediate is not formed until 300 K and skeletal oxidation does not occur until nearly 350 K. Together, the above results suggest that the vinyl hydrogen on ethylene is less reactive than the vinyl hydrogen of propylene. The methyl group attached to the vinyl carbon appears to weaken the vinyl C–H bond in propylene, causing it to break nearly 50 K before the vinyl C–H bond in ethylene.

A comparison between acetylene (dotted line) and ethylene (solid line) oxidation in 0.002 Torr of O_2 is shown in Figure 4. The two experiments differ dramatically from one another. Acetylene oxidizes in one step from approximately 310 to 420 K. As discussed previously, ethylene oxidizes in two steps, one step between 215 and 300 K and a second step between 350 and 410 K. If the ethylene oxidation intermediate between 300 and 350 K was similar to acetylene, as proposed by previous researchers, then one would expect the TP-FYNES traces would be similar above 350 K. However, above 350 K, the acetylene and ethylene traces differ significantly in both temperature and carbon concentration. This comparison of ethylene and acetylene

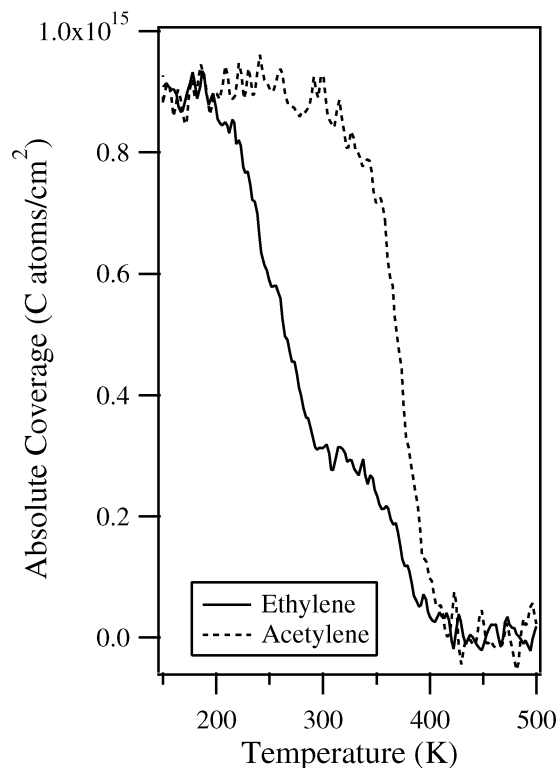


Figure 4. TP-FYNES of ethylene and acetylene in 0.002 Torr of oxygen. Acetylene oxidation proceeds without any change in stoichiometry. Intensities were measured at 330 eV.

oxidation experiments confirms that the oxidation intermediate is not acetylenic in nature.

In the following sections, the exact molecular nature of the oxidation intermediate will be further characterized and compared with FYNES experiments of known C_2H_X structures. The fitted FYNES spectra of ethylene, ethylidyne, acetylene, and the oxidation intermediate are shown in Figures 5–8. The spectra for ethylene, ethylidyne, and acetylene are included as reference standards to aid in the identification of the oxidation intermediate. When possible, the related spectra of all species were taken on the same ring fill, thus reducing any effects from changes in background scattered light. FYNES spectra were taken at two incident angles, 90° (normal) and 30° (glancing) to the surface plane. The spectra were normalized to the carbon continuum and were peak-fit as a group, using global peak-fitting criterion, including peak placement and width. Further details of spectra peak-fitting procedures and experimental conditions are outlined in the Experimental Section. The locations of all peaks for the four species are listed in Table 1.

Ethylene. FYNES spectra of ethylene taken at normal (90°) and glancing (30°) incidences are displayed in Figure 5. The concentration of the saturated ethylene FYNES spectra in Figure 5 corresponds to a coverage of 0.90×10^{15} carbon atoms/cm². The peak assignments are made by comparing similar hydrocarbon spectra found in the literature: ethylene/Pt(111),^{27–29} ethylene/Pd(111),⁴⁶ ethylene/Pd(110),⁴⁷ ethylene/Ag(110),⁴⁸ and propylene/Pt(111).³¹ The resonances observed in Figure 5 are assigned as follows: 284 eV is $C=C \pi^*$, 288 eV is $C-H \sigma^*$, and 294 eV $C=C \sigma^*$. As described in the Experimental Section, the 310 eV peak is a manifestation of division-based spectra normalization. Ethylene is reported to adsorb in a di- σ configuration with the carbon backbone nearly parallel to the surface plane as determined by NEXAFS^{27,28} and HREELS⁵ experiments. The 284 eV $C=C \pi^*$ orbital peak intensities in this current study support the nearly parallel adsorption of ethylene

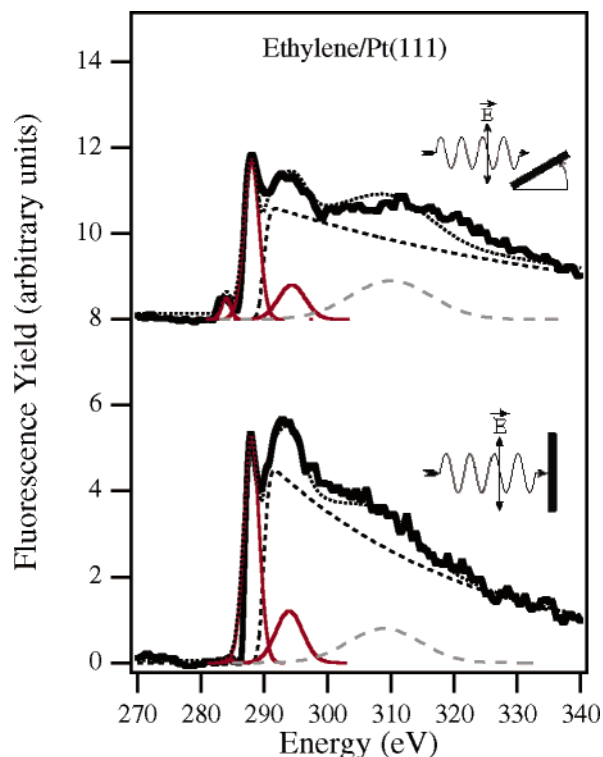


Figure 5. Normal (bottom) and glancing (top) spectra of ethylene confirming the nearly parallel, di- σ orientation on the surface. Spectra were taken at 150 K.

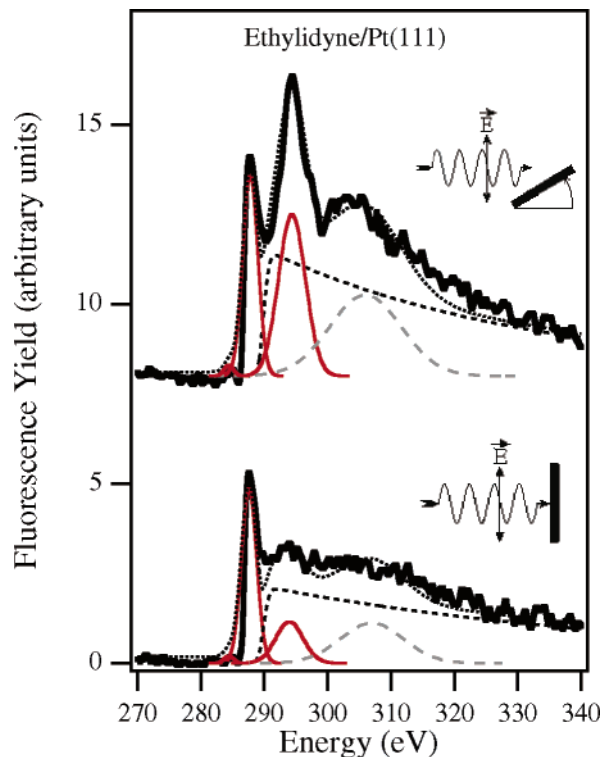


Figure 6. Normal and glancing spectra of ethylidyne. A saturated ethylene coverage was heated to 320 K under vacuum and cooled to 250 K.

on Pt(111). There is almost no $C=C \pi^*$ peak in normal incidence and a much larger π^* peak in glancing incidence, suggesting the C–C backbone is nearly parallel to the surface. Calculations comparing the intensity of the resonance ratios at the two angles are difficult due to the limited signal-to-noise ratios currently achievable. However qualitative estimates

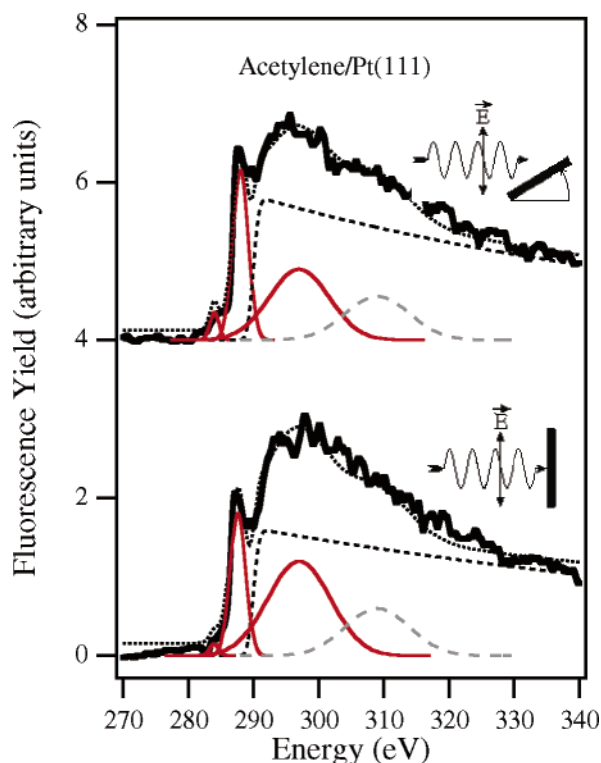


Figure 7. Normal and glancing spectra of acetylene, confirming the slightly tilted $\eta^2\text{-}\mu_3\text{-CCH}_2$ configuration on the Pt(111) surface. Spectra were taken at 150 K.

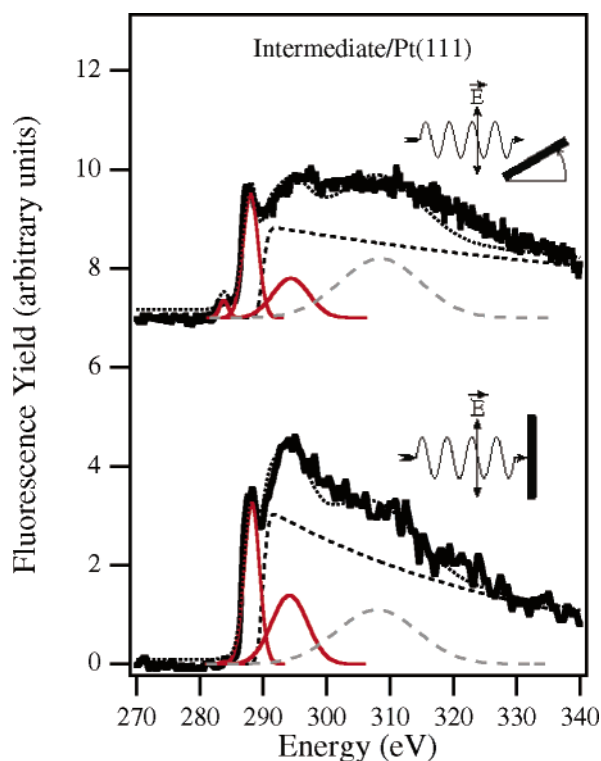


Figure 8. Normal and glancing spectra of the ethylene oxidation intermediate. A saturated coverage of ethylene was heated to 300 K in 0.002 Torr of oxygen. The oxygen was removed and the spectra were taken at 250 K.

indicate the C–C bond is tilted up slightly from the surface plane. This supports previous NEXAFS studies on Ag(110) where the authors cite a $20 \pm 5^\circ$ ethylene tilt angle.⁴⁸ Analyzing the 294.0 eV C=C σ^* intensities in normal and glancing incidences supports a similar orientation. The C=C σ^* resonance

TABLE 1: FYNES Peak Positions (eV)

| | π^* (C=C) | σ^* (C–H) | σ^* (C=C) | |
|--------------------|---------------|------------------|------------------|-----|
| ethylene | | | | |
| normal | 284.2 | 288.0 | 294.0 | 308 |
| glancing | 284.0 | 287.8 | 294.4 | 310 |
| reference: Pt(111) | 285.0 | 288.0 | 293.0 | - |
| ethynidyne | | | | |
| normal | 284.4 | 287.6 | 294.0 | 308 |
| glancing | 284.4 | 287.8 | 294.4 | 306 |
| reference: Pt(111) | 285.0 | 288.0 | 295.0 | - |
| acetylene | | | | |
| normal | 284.0 | 287.6 | 297.0 | 309 |
| glancing | 284.0 | 288.0 | 297.0 | 309 |
| intermediate | | | | |
| normal | 284.0 | 288.2 | 294.2 | 308 |
| glancing | 283.8 | 288.0 | 294.4 | 308 |

is strong in normal incidence and greatly reduced in glancing incidence. These results support the proposal that the carbon backbone is tilted up slightly from the surface plane. Exact determination of the tilt angle is limited by the uncertainty in the step function. Analysis of the 288 eV C–H σ^* resonance provides strong support for this bonding picture for ethylene on Pt(111). The C–H σ^* resonance is quite large and is located below the step edge, thus removing considerable uncertainty. Assuming a di- σ , parallel orientation for ethylene, the average olefin hydrogens would be orientated 30° from the surface plane. If all four C–H bonds make an equal contribution, the spectroscopic C–H σ^* resonance data indicate that the average C–H angle is roughly 28° . This result provides strong support for ethylene adsorbing nearly parallel to the surface. Together, peak intensities at normal and glancing incidences confirm a di- σ configuration of ethylene with the carbon backbone tilted up slightly up from the Pt surface.

Ethynidyne. The bonding and configuration of ethynidyne/Pt(111) has been verified by FYNES spectra taken at normal and glancing incidences (Figure 6). The ethynidyne layer was prepared by adsorbing ethylene at 150 K, heating the surface to 320 K, then cooling the sample to 250 K to prevent further dehydrogenation while data were collected.³ The ethynidyne coverage in Figure 6 corresponds to a coverage of 0.55×10^{15} carbon atoms/cm². Peak assignments, listed in Table 1, are based on comparisons to literature spectra of adsorbed ethynidyne on Pt(111).^{27,28,49} The 284 eV peak represents the C1 p-orbitals triple-bonded to the surface, the 288 eV peak is the C–H σ^* resonance, and the 294 eV peak is the C–C σ^* transition. As with the ethylene spectra, the 306/308 eV peak is an artifact due to division-based spectra normalization.

Analyzing the p-orbital for orientation information is difficult due to the limited signal-to-noise ratios currently available for the ethynidyne layer. Qualitatively, the p-orbital intensity is greater in glancing incidence, compared to normal incidence, supporting NEXAFS results by Horsley, Stöhr, and Koestner and the upright configuration of ethynidyne.²⁷ Examining the C–H σ^* resonances can aid in confirming the structure of ethynidyne. The C–H σ^* intensity is substantial and is well below the edge jump, thus removing any intensity ambiguity caused by placement of the step function. Assuming ethynidyne is adsorbed with the C–C axis exactly perpendicular to the surface, then the three C–H bonds would be 19.5° up from the surface plane. On the basis of these data, the C–H σ^* intensity is larger in glancing incidence than at normal incidence, suggesting a C–H angle that is orientated up from the surface plane. The average angle is roughly 23° , supporting the upright configuration of ethynidyne. Examining the 294 eV C–C σ^* peak intensities clearly indicates an upright orientation of ethynidyne. There is a dominant resonance at 294 eV in the

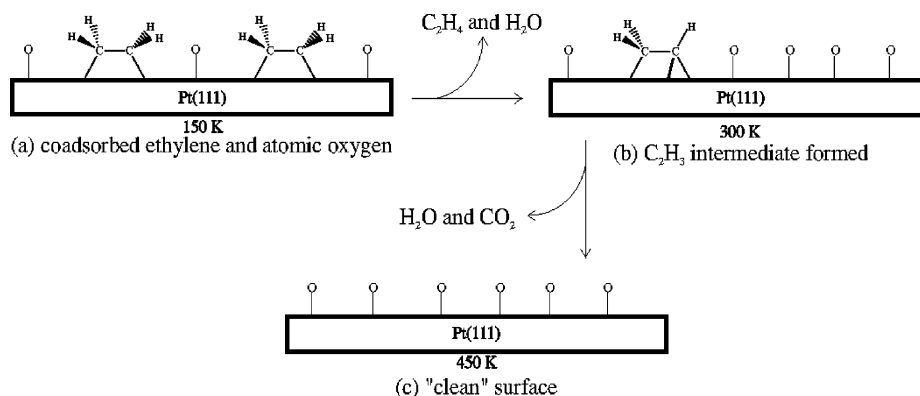


Figure 9. Mechanism of ethylene oxidation on Pt(111) with excess oxygen as it tracks with increasing surface temperature.

glancing spectrum, while there is almost no intensity in the peak at 294 eV in the normal incident spectra. As mentioned previously exact angle calculations are difficult given the overlap of the C–C resonance with the placement of the step function; however, qualitative inspection clearly shows a large angular dependence of the C–C σ^* resonance. All three main molecular resonances in Figure 6 support the perpendicular orientation of ethylidyne.

Acetylene. FYNES spectra of acetylene taken at normal (90°) and glancing (30°) incidences are shown in Figure 7 for comparison with those of the ethylene oxidation intermediate. The details concerning acetylene bonding on Pt(111) are covered elsewhere.^{1–6,29,37,50,51} Previous NEXAFS, UPS, and sum frequency generation (SFG) results indicate acetylene adsorbs tilted up from the surface plane in a η^2 - μ_3 -CCH₂ configuration.^{7,29,37,50} The main features of the acetylene spectra are assigned as follows: 284 eV is the C≡C π^* resonance, 288 eV is the C–H σ^* resonance, and 297 eV is the C≡C σ^* resonance. Again, the 309 eV peak is a manifestation of spectra normalization. The main difference between the acetylene spectra in Figure 7 and the ethylene and ethylidyne spectra in Figures 5 and 6, respectively, is location of the C–C σ^* resonance. For ethylene spectra presented here and in the literature, the C=C σ^* resonance is consistently between 292.4 and 294.4 eV. However, for acetylene shown both in this work and in previously published spectra²⁹ the C≡C σ^* transition is located at a significantly higher energy (297 eV). This difference has been ascribed to the different C–C bond lengths of ethylene and acetylene. The higher bond order will have a higher energy C–C σ^* transition.^{29,41}

Oxidation Intermediate. Previous researchers have ascribed the ethylene oxidation intermediate to an acetylenic species.¹⁶ Comparisons of the spectra in Figures 5–7 with the FYNES spectra of the ethylene oxidation intermediate clearly indicate the intermediate is not acetylene. The ethylene oxidation intermediate was created by heating a saturated coverage of ethylene (0.90×10^{15} carbon atoms/cm²) to 300 K in 0.002 Torr of oxygen. This procedure resulted in formation of 0.28×10^{15} carbon atoms/cm² of the intermediate. The oxygen was removed, and the sample was cooled to 250 K, where the spectra were taken. The peak assignments have been made on the basis of comparisons with the ethylene, ethylidyne, and acetylene spectra: 284 eV is the C–C π^* resonance, 288 eV is the C–H σ^* resonance, and 294 eV peak is the C–C σ^* resonance. As with the three other spectra, the 308 eV peak is an artifact caused by spectra normalization using division. The location and intensities of these peaks will be compared with the three reference spectra in Figures 5–7 to determine the molecular nature of the ethylene oxidation intermediate. The small

concentration of the ethylene oxidation intermediate (0.28×10^{15} carbon atoms/cm²) makes analysis of the intermediate spectra challenging, but significant spectral resolution is obtained to identify the molecular bonding nature of the intermediate.

Intensity and peak location differences clearly indicate that the oxidation intermediate is significantly different from the three reference spectra. TP-FYNES experiments comparing the C–H and carbon continuum intensity presented here indicate that the oxidation intermediate has C₂H₃ stoichiometry. This ratio is the same C–H ratio found in ethylidyne; however, as will be discussed below, the spectra for these two species are quite different. Simple visual inspection of the two sets of spectra (ethylidyne and oxidation intermediate) indicates the spectra are strikingly different, ruling out ethylidyne as the dominant oxidation intermediate.

The C–H σ^* intensity provides additional information on the intermediate structure. Comparing ethylene and the intermediate, the C–H σ^* intensities are decreased (compared to the C–C intensity) for the oxidation intermediate, supporting the dehydrogenated nature of intermediate. The C–H σ^* resonance is larger in normal incidence for the oxidation intermediate. A similar polarization dependence was observed for ethylene, but not for ethylidyne, suggesting the intermediate bonding is similar to that of ethylene with a different C–H stoichiometry. Calculations using the peak areas at the two angles indicate a 28° C–H bond angle for the intermediate. Recall, the C–H bond angle for ethylene was also 28°.

Comparisons of the C–C σ^* resonance intensity result in clear differentiation between the four spectra. The polarization dependence of C–C σ^* resonance for the intermediate suggests that the C–C bond is orientated nearly parallel to surface plane. This is in sharp contrast to the C–C σ^* intensities found for the ethylidyne spectra. For ethylidyne, there is a large C–C σ^* peak in glancing incidence with a very small peak in normal incidence, clearly indicating a perpendicular C–C bond. However, for the intermediate, there is a large peak at 294 eV in normal incidence with a greatly reduced intensity at glancing incidence, indicating a nearly parallel C–C orientation. This clearly rules out ethylidyne as the oxidation intermediate.

Acetylene has a different stoichiometry than the intermediate, and the location of the C–C σ^* resonance is at 297 eV for acetylene, while the C–C σ^* resonance of the ethylene oxidation intermediate is at 294 eV. Together with the C₂H₃ intermediate stoichiometry determined by TP-FYNES studies at the magic angle, the location of the C–C σ^* resonance clearly eliminates the acetylenic intermediate proposed previously.¹⁶

The results presented above indicate that the intermediate has a C₂H₃ stoichiometry with bonding similar to that of ethylene on Pt(111). On the basis of these results, a tri- σ vinyl species

appears to be the dominant oxidation intermediate for ethylene. A carbon–platinum bond replaces the loss of one carbon–hydrogen bond. An analogous intermediate has been observed during propylene oxidation on Pt(111), where the vinyl hydrogen is removed, creating a tri- σ 1-methylvinyl species.³¹ In the ethylene intermediate, the C–C bond remains nearly parallel to the surface (as indicated by the C–C σ^* intensities in Figure 8), so the C–H bonds would be at a 30° angle from the surface, as in ethylene. The close agreement of the 28° calculated C–H angle for the oxidation intermediate supports this tri- σ vinyl species.

Mechanism. Both TP-FYNES and FYNES experiments suggest the mechanism for ethylene oxidation in excess oxygen illustrated in Figure 9. The diagram tracks the oxidation mechanism as a function of surface temperature. To begin, at 150 K the surface is covered with the nearly parallel, di- σ bonded ethylene (Figure 9a). As the surface temperature increases to 300 K, ethylene and water desorb from the surface, leaving a small concentration of the dehydrogenated, tri- σ vinyl intermediate and atomic oxygen on the surface (Figure 9b). Further heating to 375 K (Figure 9c) causes skeletal oxidation of the C₂H₃ intermediate, indicated by CO₂ and H₂O formation determined via TPRS.^{16,17} Finally, all surface carbon is oxidized by 450 K, leaving a “clean” platinum surface covered with atomic oxygen only (Figure 9d). This mechanism is valid over an extremely wide range of oxygen pressures, from vacuum up to 0.01 Torr.

Conclusions

The oxidation of ethylene on the Pt(111) surface was characterized in oxygen pressures up to 0.01 Torr using a combination of spectroscopic and temperature-programmed techniques. The reaction proceeds via an intermediate, which is stable over a 40 K temperature range. Magic angle TP-FYNES experiments at the C–H σ^* resonance and in the carbon continuum indicate oxydehydrogenation precedes skeletal oxidation, producing a C₂H₃ intermediate at 300 K. Comparisons of the intermediate FYNES spectra with ethylene, ethylidyne, and acetylene reference FYNES spectra indicate a tri- σ vinyl intermediate. Further oxidation causes skeletal oxidation of this intermediate, leaving a carbon-free platinum surface by 415 K.

Acknowledgment. Financial support was provided by DOE Grant DE-FG02-91ER1490. This research was carried out at the National Synchrotron Light Source, Brookhaven National Laboratory, which is supported by the U.S. Department of Energy, Division of Materials Sciences and Division of Chemical Sciences, under Contract No. DE-AC02-98CH10886. Certain commercial names are identified in this paper for the purpose of clarity in the presentation. Such identification does not imply endorsement by the National Institute of Standards and Technology.

References and Notes

- (1) Stair, P. C.; Somorjai, G. A. *J. Chem. Phys.* **1977**, *66*, 2036.
- (2) Kesmodel, L. L.; Dubois, L. H.; Somorjai, G. A. *J. Chem. Phys.* **1979**, *70*, 2180.
- (3) Salmeron, M.; Somorjai, G. A. *J. Phys. Chem.* **1982**, *86*, 341.
- (4) Koestner, R. J.; Frost, J. C.; Stair, P. C.; Van Hove, M. A.; Somorjai, G. A. *Surf. Sci.* **1982**, *116*, 85.
- (5) Ibach, H.; Lehwald, S. *J. Vac. Sci. Technol.* **1978**, *15*, 407.
- (6) Demuth, J. E. *Surf. Sci.* **1979**, *84*, 315.
- (7) Felter, T. E.; Weinberg, W. H. *Surf. Sci.* **1981**, *103*, 265.
- (8) Kubota, J.; Ichihara, S.; Kondo, J. N.; Domen, K.; Hirose, C. *Surf. Sci.* **1996**, *357–358*, 634.
- (9) Griffiths, K.; Lennard, W. N.; Mitchell, I. V.; Norton, P. R. *Surf. Sci. Lett.* **1993**, *284*, L389.
- (10) Freyer, N.; Pirug, G.; Bonzel, H. P. *Surf. Sci.* **1983**, *125*, 327.
- (11) Mitchell, I. V.; Lennard, W. N.; Griffiths, K.; Massoumi, G. R.; Huppertz, J. W. *Surf. Sci. Lett.* **1991**, *256*, L598.
- (12) Yata, M.; Madix, R. J. *Surf. Sci.* **1995**, *328*, 171.
- (13) Kua, J.; Goddard, W. A. *J. Chem. Phys.* **1998**, *102*, 9492.
- (14) Tsai, Y.-L.; Xu, C.; Koel, B. E. *Surf. Sci.* **1997**, *385*, 37.
- (15) Windham, R. G.; Bartram, M. E.; Koel, B. E. *J. Phys. Chem.* **1988**, *92*, 2862.
- (16) Berlowitz, P.; Megiris, C.; Butt, J. B.; Kung, H. H. *Langmuir* **1985**, *1*, 206.
- (17) Steininger, H.; Ibach, H.; Lehwald, S. *Surf. Sci.* **1982**, *117*, 685.
- (18) Cassuto, A.; Mane, M.; Hugenschmidt, M.; Dolle, P.; Jupille, J. *Surf. Sci.* **1990**, *237*, 63.
- (19) Palmer, R. L. *J. Vac. Sci. Technol.* **1975**, *12*, 1403.
- (20) Ackelid, U.; Wallenberg, L. R.; Petersson, L.-G. *Catal. Lett.* **1996**, *39*, 129.
- (21) Vayenas, C. G.; Lee, B.; Michaels, J. J. *Catal.* **1980**, *66*, 36.
- (22) Ackelid, U.; Olsson, L.; Petersson, L.-G. *J. Catal.* **1996**, *161*, 143.
- (23) Harkness, I. R.; Hardacre, C.; Lambert, R. M.; Yentekakis, I. V.; Vayenas, C. G. *J. Catal.* **1996**, *160*, 19.
- (24) Hiam, L.; Wise, H.; Chaikin, S. J. *Catal.* **1968**, *10*, 272.
- (25) Schwartz, A.; Holbrook, L. L.; Wise, H. J. *Catal.* **1971**, *21*, 199.
- (26) Velic, D.; Levis, R. J. *J. Chem. Phys.* **1996**, *104*, 9629.
- (27) Horsley, J. A.; Stöhr, J.; Koestner, R. J. *J. Chem. Phys.* **1985**, *83*, 3146.
- (28) Koestner, R. J.; Stöhr, J.; Gland, J. L.; Horsley, J. A. *Chem. Phys. Lett.* **1984**, *105*, 332.
- (29) Stöhr, J.; Sette, F.; Johnson, A. L. *Phys. Rev. Lett.* **1984**, *53*, 1684.
- (30) Cassuto, A.; Mane, M.; Tourillon, G.; Parent, P.; Jupille, J. *Surf. Sci.* **1993**, *287/288*, 460.
- (31) Gabelnick, A. M.; Capitano, A. T.; Kane, S. M.; Gland, J. L.; Fischer, D. A. *J. Am. Chem. Soc.* **2000**, *122*, 143.
- (32) Masson, F.; Sass, C. S.; Grizzi, O.; Rabalais, J. W. *Surf. Sci.* **1989**, *221*, 299.
- (33) Yu, R.; Gustafsson, T. *Surf. Sci.* **1987**, *182*, L234.
- (34) Gabelnick, A. M.; Gland, J. L. *Surf. Sci.* **1999**, *440*, 340.
- (35) Burnett, D. J.; Gabelnick, A. M.; Marsh, A. L.; Fischer, D. A.; Gland, J. L. *Surf. Sci.* **2004**, *553*, 1.
- (36) Gabelnick, A. M.; Burnett, D. J.; Gland, J. L.; Fischer, D. A. *J. Phys. Chem. B* **2001**, *105*, 7748.
- (37) Burnett, D. J.; Gabelnick, A. M.; Fischer, D. A.; Marsh, A. L.; Gland, J. L. *J. Catal.* **2005**, *230*, 291.
- (38) Franz, A. J.; Ranney, J. T.; Gland, J. L.; Bare, S. R. *Surf. Sci.* **1997**, *374*, 162.
- (39) Fischer, D. A.; Colbert, J.; Gland, J. L. *Rev. Sci. Instrum.* **1989**, *60*, 1596.
- (40) Gland, J. L.; Somorjai, G. A. *Adv. Colloid Interface Sci.* **1976**, *5*, 205.
- (41) Stöhr, J. *NEXAFS Spectroscopy*; Springer-Verlag: New York, 1992.
- (42) Outka, D. A.; Stöhr, J. *J. Chem. Phys.* **1988**, *88*, 3539.
- (43) Norton, P. R.; Davies, J. A.; Jackman, T. E. *Surf. Sci.* **1982**, *122*, L593.
- (44) Redhead, P. A. *Vacuum* **1962**, *12*, 203.
- (45) Gland, J. L. *Surf. Sci.* **1980**, *93*, 487.
- (46) Wang, L. P.; Tysoe, W. T.; Ormerod, R. M.; Lambert, R. M.; Hoffmann, H.; Zaera, F. *J. Phys. Chem.* **1990**, *94*, 4236.
- (47) Okuyama, H.; Ichihara, S.; Ogasawara, H.; Kato, H.; Komeda, T.; Kawai, M.; Yoshinobu, J. *J. Chem. Phys.* **2000**, *112*, 5948.
- (48) Solomon, J. L.; Madix, R. J.; Stöhr, J. *J. Chem. Phys.* **1990**, *93*, 8379.
- (49) Koestner, R. J.; Van Hove, M. A.; Somorjai, G. A. *J. Phys. Chem.* **1983**, *87*, 203.
- (50) Cremer, P. S.; Su, X.; Shen, Y. R.; Somorjai, G. A. *J. Phys. Chem. B* **1997**, *101*, 6474.
- (51) Kesmodel, L. L.; Baetzold, R. C.; Somorjai, G. A. *Surf. Sci.* **1977**, *66*, 299.